



Research Article

Impact of measles virus infection on immune signaling pathways in human lung cancer cell lines

Shiful Islam ^{1,*} and Muhammad Tarek ¹¹ Department of Biotechnology, Faculty of Natural Science, Norwegian University of Science and Technology, Trondheim 7491, Norway.

* Correspondence: saifparvez95@gmail.com (S.I.)

Citation: Islam S. and Tarek M. Impact of measles virus infection on immune signaling pathways in human lung cancer cell lines. *Jour. Bas. Sci.* 2025, 1(5). 1-13.

Received: February 15, 2025

Revised: February 28, 2025

Accepted: March 04, 2025

Published: March 11, 2025

doi: 10.63454/jbs20000011

ISSN: XXXX-XXXX

Abstract: The measles virus is an aerosol-transmitted virus that kills a considerable number of people and infects a lot of youngsters every year. It was formerly thought to replicate in the respiratory epithelium before spreading, however it was recently demonstrated to use signaling lymphocytic activation molecule family member 1 as a receptor to first infect macrophages and dendritic cells of the airways. After passing through the respiratory epithelium, these cells carry the infection to lymphatic organs where the measles virus multiplies rapidly. Thus, we decided to selected the publicly available dataset which are related to measles infection where we had seven different types of cell lines and performed in-silico analysis of the gene expression patterns and the altered signaling pathways and finally, compared them between the cell lines. The potential focus of the study was to understand the impact on immune signaling pathways and their components. Here, we observe that there are a significant number of genes and the pathways potentially altered as a result of measles infection. Based on our results, we conclude that APC, RAP1, NK cell, cAMP, RAS, TNF, and neuroactive ligand-receptor signaling are among the leading altered pathways.

Keywords: Measles virus; Lung Cancer; cell lines; gene expression profiling; pathway analysis

1. Introduction

Lung cancer is a type of cancer that begins as lung cell proliferation. Breathing is controlled by the lungs, two spongy organs in the chest. The most common cause of cancer-related fatalities globally is lung cancer. Lung cancer is most likely to strike smokers. The more cigarettes smoked over an extended period of time, the higher the risk of lung cancer. Giving up smoking dramatically reduces the risk of lung cancer, even if you have smoked for a long time. Individuals who have never smoked may also develop lung cancer. Lung carcinoma, another name for lung cancer, is a type of malignant tumor that starts in the lung[1-4]. Genetic damage to the DNA of airway cells, frequently brought on by cigarette smoking or harmful chemical inhalation, is the cause of lung cancer. A tumor can arise as a result of damaged airway cells having the capacity to proliferate unchecked. Tumors spread throughout the lung and impair lung function if left untreated. Lung tumors eventually spread to other areas of the body through metastasis. Only medical imaging can identify early-stage lung cancer, which frequently exhibits no symptoms. The majority of patients have nonspecific respiratory issues, such as coughing, dyspnea, or chest pain, as the malignancy worsens. The tumor's size and location determine further symptoms. In order to identify the location and size of any tumors, people who are suspected of having lung cancer usually go through a battery of imaging examinations. A biopsy of the suspected tumor must be viewed under a microscope by a pathologist in order to make a definitive diagnosis of lung cancer. A pathologist can identify malignant cells and categorize the tumor based on the cells from which it originates. Small-cell lung cancer (SCLC) accounts for about 15% of instances, while adenocarcinomas, squamous-cell carcinomas, and large-cell carcinomas make up the remaining 85% of cases, often known as non-small-cell lung cancers, or NSCLC[5]. Following diagnosis, further imaging and biopsies are performed to assess the extent of the cancer's spread and define its stage.

Environmental exposure to cooking fumes and tobacco smoke, air pollution, radon, occupational carcinogens, underlying nonmalignant lung illness, immunologic dysfunction, and genetic predisposition are additional significant risk factors for the development of lung cancer. Although it has been suggested, a viral etiology for lung cancer is still up for debate. Human papillomavirus (HPV), Epstein-Barr virus (EBV), simian virus 40 (SV40), BK virus, JC virus, and human cytomegalovirus (HCMV) are among the viruses that have been proposed. The aerosol-transmitted virus known as measles (MV) kills about 120,000 people year and infects about 10 million youngsters. It was recently demonstrated to first infect macrophages and dendritic cells of the airways using the signaling lymphocytic activation molecule (SLAM,

CD150) as a receptor, despite the long-held belief that it was replicated in the respiratory epithelium. These cells then transport the virus to lymphatic organs, where MV multiplies rapidly, after passing through the respiratory epithelium. We still don't know how or where the virus re-enters the airways. According to Leonard VHJ et al. (2008)[6], some cancer cell lines, however, have been reported to be either permissive for wt MV infection or not. Furthermore, although it has not been discovered in humans, the Jaagsiekte sheep retrovirus-related retrovirus has been linked to bronchioloalveolar cancer in sheep. A recent study suggested that measles virus (MV) may be linked to the etiology of Hodgkin's lymphoma, and there are a few instances in the literature suggesting that MV may be linked to lung cancer[7-10]. A common RNA virus is measles. Numerous persistently infected cell lines have been studied, and it may result in a persistent viral infection. It has been proposed that the wild-type virus cannot cause persistent infection; only the modified virus can. Pirh2 has been discovered to be overexpressed in lung cancer samples in comparison to normal lung tissue, and MV phosphoprotein may prevent Pirh2 from ubiquitinating p53, the cell cycle regulator. Furthermore, lung cancer cells overexpress CD46, a cell membrane complement inhibiting protein that functions as an MV receptor. The current investigation sought to ascertain whether MV may be found in patient biopsies for non-small cell lung cancer (NSCLC). Additionally, we looked at a number of clinicopathological and demographic characteristics in NSCLC patients and how they related to the tumor tissue's expression of p53, Pirh2, and MV antigens[11].

Proto-oncogenes (genes that promote cell growth, which can become oncogenes due to mutation) and suppressor genes (genes encoding proteins, whose function is to inhibit cell growth and differentiation and to maintain cell stability; mutations in these genes lead to uncontrolled cell proliferation) are significantly impacted by genetic aberrations and epigenetic changes that occur in the human body. These changes facilitate the development and migration of cancer cells. But this is just one part of the procedure. The immune system has a very significant capacity to track, identify, and eliminate cancer cells when homeostasis is maintained. Nevertheless, these cells have evolved a number of defenses that enable them to evade immune system surveillance. Thus, any disruptions in the human body that affect how the immune system functions ought to be regarded as the second possible mechanism in the etiology of cancer, including lung cancer[1, 4, 12-22].

In this study, we have selected the gene expression dataset (GSE32155[23]) from gene expression omnibus (GEO) which publicly available (<https://www.ncbi.nlm.nih.gov/geo/query/acc.cgi?acc=GSE32155>) for different lung cancer cell lines and performed gene expression profiling. Afterwards, we predicted the enriched pathways for the differentially expressed genes (DEGs). Finally, we exclusively selected the immune signaling pathways and the DEGs belonging to immune system and evaluated them.

2. Methods

2.1. Data collection: The gene expression dataset (GSE32155[23]) for various lung cancer cell lines was chosen for this work from the Gene Expression Omnibus (GEO)[24], which is publicly available (<https://www.ncbi.nlm.nih.gov/geo/query/acc.cgi?acc=GSE32155>). The 21 samples in the collection dataset are split up into seven sample groups, each of which represents three biological replicates of one of the seven cell lines.

Gene expression profiling was then carried out. The enriched pathways for the differentially expressed genes (DEGs) were then predicted. To consider the genes as DEGs, we have two parameters fold change and p-value. The gene which have fold change ≥ 2.0 and p-value ≤ 0.05 then we considered as up-regulated and the gene with fold change ≤ -2.0 and p-value ≤ 0.05 we considered as down-regulated gene. Lastly, we assessed the immune system's DEGs and immunological signaling pathways that we specifically chose. In pathway analysis, we only considered those pathways which have p-values ≤ 0.05 as enriched pathways. In this case, we have seen that there were large number of genes within these ranges so to be more strict, we decided to include the top DEGs (approximately 200 up and down regulated genes) for the study[25-27].

2.2. Data processing and analysis: First of all, we have prepared the group names for different cell lines and utilized the in-built tool GEO2R[24] at GEO webpage to predict the fold change and p-values for all the genes. We compared one group with another group to predict the DEGs between two groups as shown in Figure 1. Furthermore, GECIP toolbox[28] was

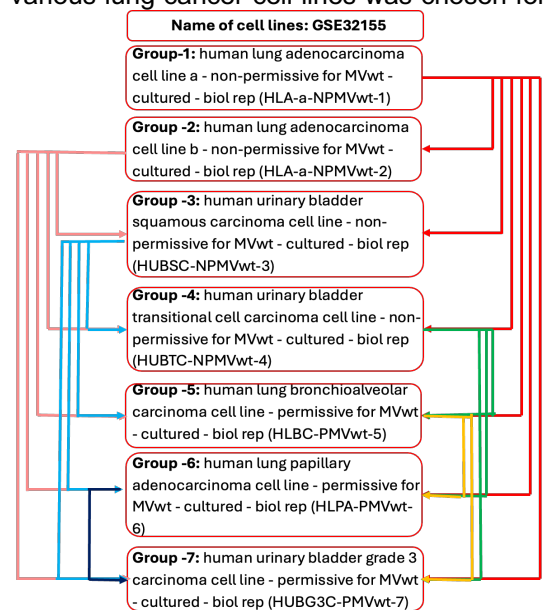
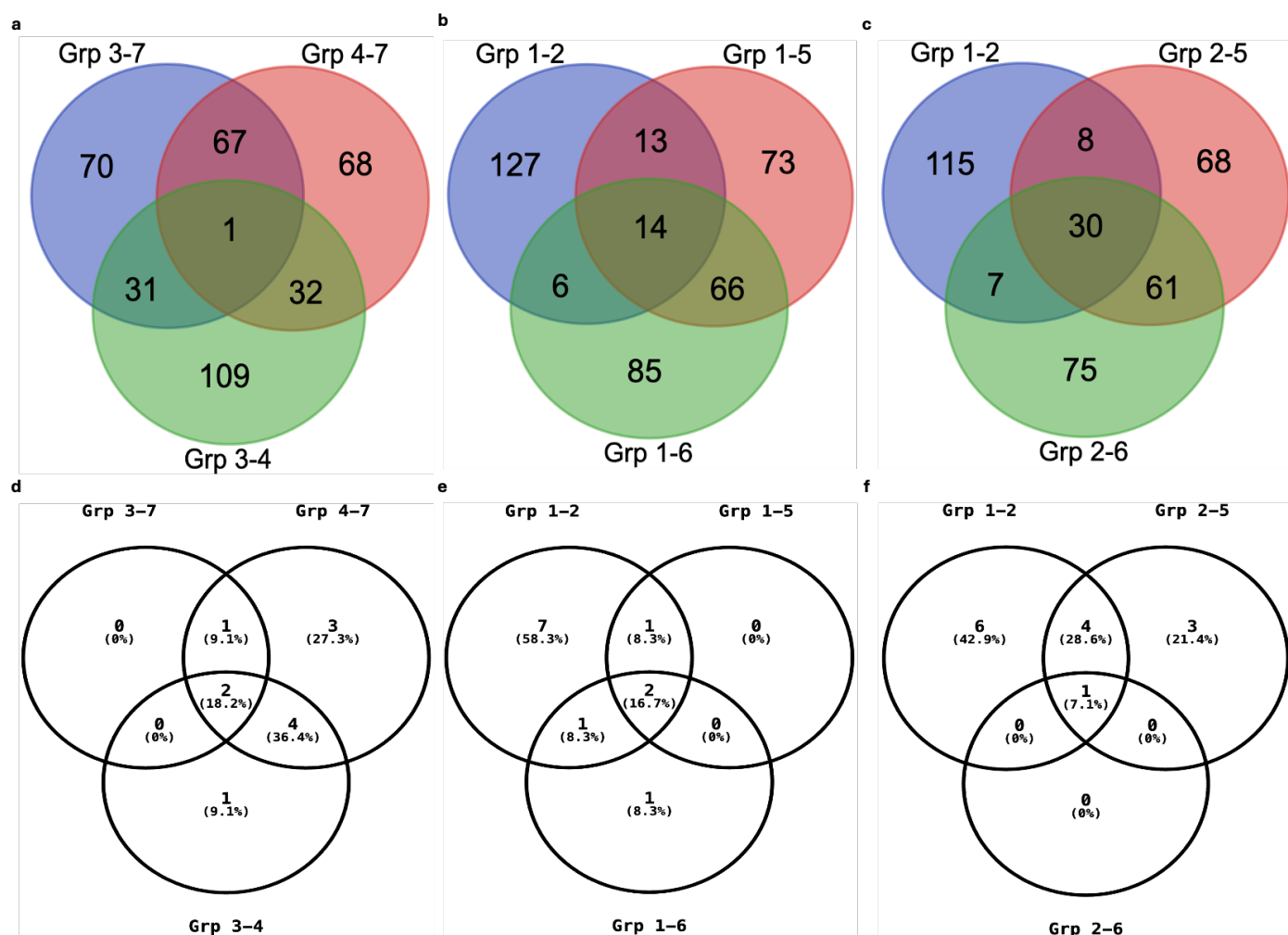


Figure 1. Grouping of the samples and its comparison for predicting DEGs between two groups.

used for predicting the enriched pathways. After predicting the DEGs and enriched pathways, we mapped out all the DEGs belonging to the immune system/signaling pathways[13, 25, 26, 29-31]. For venn diagram, we used venny tool which is online available at this link: <https://bioinfogp.cnb.csic.es/tools/venny/>.

3. Results

3.1. Gene expression profiling to predict cell line specific genes: We performed the gene expression analysis of all the seven cell lines and selected top 200 DEGs (100 up and 100 down) and afterwards plotted venn diagram to show the number of genes common between different groups or cell lines. For the detailed grouping, we presented the description in Figure 1. In the first step, we compared the top 200 DEGs of group 3-7, group 4-7, and group 3-4 where we observed that 67 DEGs were common between group 3-7 and group 4-7, 31 DEGs were common between group 3-7 and group 3-4, 32 DEGs were common between group 4-7 and group 3-4 while there was only one DEG common between all the three DEGs list. 70, 68, and 109 DEGs were group specific DEGs for group 3-7, group 4-7, and group 3-4, respectively (Figure 2a). Similarly, we compared the top 200 DEGs of group 1-2, group 1-5, and group 1-6 where we observed that 13 DEGs were common between group 1-2 and group 1-5, 6 DEGs were common between group 1-2 and group 1-6, 66 DEGs were common between group 1-5 and group 1-6 while there were 14 DEGs common between all the three DEGs list. 127, 73, and 85 DEGs were group specific DEGs for group 1-2, group 1-5, and group 1-6, respectively (Figure 2b). Again, we compared the top 200 DEGs of group 1-2, group 2-5, and group 2-6 where we observed that 8 DEGs were common between group 1-2 and group 2-5, 7 DEGs were common between group 1-2 and group 2-6, 61 DEGs were common between group 2-5 and group 2-6 while there were 30 DEGs common between all the three DEGs list. 115, 68, and 75 DEGs were group specific DEGs for group 1-2, group 2-5, and group 2-6,



respectively (Figure 2c).

Figure 2. Gene expression profiling and pathway enrichment analysis. (a) Human urinary bladder squamous carcinoma cell line - non-permissive for MVwt (Grp 3) , human urinary bladder transitional cell carcinoma cell line - non-permissive for MVwt (Grp 4), and human urinary bladder grade 3 carcinoma cell line - permissive for MVwt (Grp 7). (b) Human lung adenocarcinoma cell line a - non-permissive for MVwt (Grp 1), human lung

adenocarcinoma cell line b - non-permissive for MVwt (Grp 2), human lung bronchioalveolar carcinoma cell line - permissive for MVwt (Grp 5), and human lung papillary adenocarcinoma cell line - permissive for MVwt (Grp 6). (c) Human lung adenocarcinoma cell line a - non-permissive for MVwt (Grp 1), human lung adenocarcinoma cell line b - non-permissive for MVwt (Grp 2), human lung bronchioalveolar carcinoma cell line - permissive for MVwt (Grp 5), and human lung papillary adenocarcinoma cell line - permissive for MVwt (Grp 6). (d), (e), and (f) are comparative analysis of the enriched pathways for the respective groups as mentioned in (a), (b), and (c), respectively.

3.2. Evaluation of functional impact: After gene expression profiling, we performed pathway enrichment analysis and compared the different groups similar to the gene expression comparative analysis. Here, we observed that one pathway was common between group 3-7 and group 4-7, no pathway was common between group 3-7 and group 3-4, four pathways were common between group 4-7 and group 3-4 while there were two pathways common between all the three pathways list. zero, three, and one pathways were group specific pathways for group 3-7, group 4-7, and group 3-4, respectively (Figure 2d). Similarly, we compared the enriched pathways of group 1-2, group 1-5, and group 1-6 where we observed that one pathway was common between group 1-2 and group 1-5, one pathway were common between group 1-2 and group 1-6, zero pathway was common between group 1-5 and group 1-7 while there were two pathways common between all the three pathways list. Seven, zero, and one pathways were group specific pathways for group 1-2, group 1-5, and group 1-6, respectively (Figure 2e). Again, we compared the enriched pathways of group 1-2, group 2-5, and group 2-6 where we observed that four pathways were common between group 1-2 and group 2-5, zero pathways were common between group 1-2 and group 2-6, zero pathways were common between group 2-5 and group 2-7 while there was one pathway common between all the three pathways list. Six, three, and zero pathway were group specific pathways for group 1-2, group 2-5, and group 2-6, respectively (Figure 2f).

3.3. Comparative analysis of the DEGs predicts potentially significant immune signaling genes: The analysis of human urinary bladder squamous carcinoma cell line (non-permissive for MVwt (Grp 3)), human urinary bladder transitional cell carcinoma cell line (non-permissive for MVwt (Grp 4)), and human urinary bladder grade 3 carcinoma cell line (permissive for MVwt (Grp 7)) predicted the significant number of genes associated with immune system. These immune systems-associated genes are group-specific as well as common between two groups. Similar to it, we performed the comparative analysis of the genes for the other two groups subset according to the venn diagrams (Figure 2a, 2b, 2c)) (Table 1). These two subgroups were (a) human lung adenocarcinoma cell line a - non-permissive for MVwt (Grp 1), human lung adenocarcinoma cell line b - non-permissive for MVwt (Grp 2), human lung bronchioalveolar carcinoma cell line - permissive for MVwt (Grp 5), and human lung papillary adenocarcinoma cell line - permissive for MVwt (Grp 6) (Table 2) and (b) human lung adenocarcinoma cell line a - non-permissive for MVwt (Grp 1), human lung adenocarcinoma cell line b - non-permissive for MVwt (Grp 2), human lung bronchioalveolar carcinoma cell line - permissive for MVwt (Grp 5), and human lung papillary adenocarcinoma cell line - permissive for MVwt (Grp 6) (Table 3).

Table 1. Representation of outcome of Figure 2a i.e., the total number of genes and the names of genes for the groups selected to draw it.

List names	Number of genes	Number of unique genes
Grp 3-4	198	173
Grp 3-7	198	169
Grp 4-7	199	169
Overall number of unique genes		379
Names	Total	genes
Grp 3-4 Grp 3-7 Grp 4-7	1	UNK (unknown/un-annotated gene)
Grp 3-7 Grp 4-7	67	IL7R MPDZ FLRT3 GDPD2 BNIP3 MAP1B ZSCAN18 RBMS3 GTSF1 SSX4B GAGE3 CRACR2A MSN DSCR8 CHP2 NRP1 CDH13 HOXB9 MGAT3 HSD3B1 INHBA HIPK2 XAGE2 ANXA10 LGSN CCBE1 ST8SIA6-AS1 PAGE5 THSD7A HOXC9 FAM9C FOXA1 GAGE7 PLCXD3 CRYAB PAGE2 CCK SSX7 HOXB3 LARP6 BEX4 LOC101060157 MAPK4 CDH2 LAMB4 LINC01116 HOXA7 PRSS23 CPPED1 CGA CXCL1 HOXB6 DAPK1 PRKCA GJA5 ANTXR2 ARSJ CRNDE HMGA2 TOX2 VGLL1 SPOCD1 PAGE2B RPL39L MECOM TMEM246 CRCT1

Grp 3-4 Grp 3-7	31	MAGEH1 HSD17B2 LUM MMP7 RTP3 FAP IRX4 IGF2 KLF8 IQCA1 ZNF613 IFNK RPS4Y2 SGCE TSHZ3 SRGN ALDH7A1 PEG10 RPS4Y1 RBP1 MLPH MMP10 LINC00116 IRX2 MMP1 HCAR1 MGST1 FLRT2 ACKR3 PLAGL1 C12orf54
Grp 3-4 Grp 4-7	32	HOXD3 KCNQ1OT1 COL4A2 COL6A2 WSCD1 CXCL6 EPN3 AADAC SHISA3 TMEM30B KLK8 OVOL1 COL6A1 CDH1 FLI1 SMR3B TRIM29 WNT10A RAB25 LAD1 KLK5 KCNJ15 TMEFF2 S100A8 CDH4 DAPP1 MFAP5 VAV3 NEURL1 DPYSL3 ABCB1 S100A9
Grp 3-7	70	XAGE3 PLCE1 SPEG KRT19 RAB38 CAPN6 FSTL5 NPFFR2 SEMG1 NTSR1 WISP2 KRT24 MMP13 CTAG1A GLIPR1 ZIC1 LOX FAM43B TNC TGFB3 SLCO1B3 FRY KCNIP3 APCDD1L EIF5A2 C6orf141 CT83 KBTBD11 CD200 S1PR1 C5orf38 GPR161 SULF2 DNAJA4 PLAC4 FUT9 SOD3 PLIN2 MXRA5 FOXL2 GPR68 FOXF2 SNCA CLIC5 PTHLH QPRT INSL4 VCX PNMA3 VCX3A RIPPLY3 POPDC3 AMOT NRG1 CHST6 SXX1 NRP2 COX7B2 SGIP1 DLL1 GALNT18 CTAG2 VCX2 HOXA9 ABCA13 NDN BNC1 MUC15 ZNF595 FAM133A
Grp 4-7	69	TLR4 CCNA1 HOXB5 ALDH1A3 GPR158 HOXB8 DPF3 SMOX NCKAP5 COL5A2 ANKRD22 ALOX5 VIM S100A14 SPRR3 UPK1B ASCL2 PRSS12 TNNT2 EDNRB GPX7 NLRP7 HOOK1 ZNF704 KLK7 ID4 LOC283454 FBN2 ABR SMIM22 S100A7 DZIP1 KLF12 KIAA1211L ALDH3A1 CALB2 NECTIN4 CNIH3 TSPAN8 IGFBP4 PTX3 FGF2 COL18A1 TMC5 BSPRY HPGD FAM20C SPRR1A RECK F2R MAL TMEM125 SYT8 HOXB13 COL1A2 BICC1 COL8A1 IGFBP5 CLDN7 CD70 LYPD1 RBPMS EYA2 IRX3 CCDC88A MYADM ANXA9 SPINK5

Grp 3-4	109	<p>C3orf14 FARP1 CDH3 FAM84A CSTA GREM2 EPS8L1 TRPV2 HOXC13-AS ANXA6 NID1 TMEM47 APBA2 PKP1 ZNF93 SPINK6 SESN3 CNRIP1 FGFR1 DSC3 FAM101A AFAP1-AS1 KRT27 CD24 CALB1 ZNF347 B4GALNT4 RGL3 SERPINB13 CSF3 UGT1A8 AK5 C5orf46 NRXN3 TMPRSS4 HS6ST2 PAX6 SCG2 PPP1R3C NETO1 ABCA6 LRCH2 ZNF671 KRT5 CXorf57 TTC28 NLRP2 SERPINB4 NRG2 KRT6C LOC105379362 WNT4 ZNF818P SLCO2A1 KRT6B DDX3Y SENCN SPARC COL5A1 OVOL2 NPNT IL24 XIST RNF43 PRAME PPP1R9A SERP2 LINC00165 G0S2 CBLC RASSF2 SERPINB3 GALNT5 FYB TMTC1 PICSAR MUC4 C1orf116 AUTS2 VSNL1 CA2 RNF128 TENM2 KRT6A ZNF829 KIF5C P3H3 PABPC4L C17orf51 MAGI2-AS3 HSPA12A MMP12 SOX2 ARM CX2 TP63 CMTM7 METTL7A GRHL2 MAGEA9 GNG11 TNFSF12 DSG3 MAGEA4 KRT7 CACNA2D3 FAM174B MOB3B SYBU COL17A1</p>
---------	-----	--

Table 2. Representation of outcome of Figure 2b i.e., the total number of genes and the names of genes for the groups selected to draw it.

List names	Number of genes	Number of unique genes
Grp 1-2	198	160
Grp 1-5	197	166
Grp 1-6	198	171
Overall number of unique elements		384
Names	Total	Genes
Grp 1-2 Grp 1-5 Grp 1-6	14	CYB5R2 COL4A5 UNK CCND2 CRH SEC14L4 SCOC ST8SIA6-AS1 DNAJA4 FOXF2 CX3CL1 SCEL PDE4B AGR2
Grp 1-2 Grp 1-5	13	LEF1 GRAMD1B CCL20 UTS2 SOX17 CDH10 TFPI2 HOXB3 PRKCQ-AS1 NNMT GSTT1 GNG11 SPOCK1
Grp 1-2 Grp 1-6	6	KCNMA1 DMD TMEM30B CSGALNACT1 GPX1 MAGEA4

Grp 1-5 Grp 1-6	66	SYTL5 COL4A6 HDGFRP3 LAMB3 CHGB KCNG1 MICU3 NPTX2 DNM3 TMEM45B FLJ35934 AFAP1-AS1 MAGED4B TRIML2 BST2 GCNT3 KCNB1 SP100 CLDN4 ANTXR1 UBXN10 BMP7 PLAT AIM2 SMIM22 NEFH HS3ST1 DZIP1 SULF2 BEX3 SYK ADGRF1 ERP27 SRGN KCNQ2 ASRGL1 AKAP12 PXDN ELF3 RAB25 LAMA1 LAD1 CST6 TACSTD2 CACNG7 ATCAY LHX2 MUC4 C1orf116 PNMAL1 TGFBI HOXB13 LY96 SFRP1 SELENBP1 HTRA1 OLFM1 HCAR1 CLDN7 PRRX2 IGF2BP1 ATP10A RAB39B KRT7 HOPX TMEM246
Grp 1-2	127	EMP1 ERBB4 CYP26A1 COL3A1 SLC39A8 KCNQ1OT1 PAM STYK1 TM4SF1 CDH7 NTSR1 C15orf48 CTAG1A SULF1 ZNF93 FBLL1 ZDHHC15 SGK1 CD24 SSPN TMEM35A TUNAR KIAA2022 MBP ZNF667-AS1 PCDH11Y SOSTDC1 BASP1 FAXDC2 SOX21 KIRREL ZNF439 GSG1 ARL14 PRL LIN7A TEK PDLIM3 ZNF702P PROK2 CDCP1 IQCA1 TCEAL7 NNT UTS2B RGS17 SAT2 CXCL2 CLDN1 VWA5A RGCC ZNF736 ZNF257 S1PR1 LOC645321 FAM9C FGF9 FRRS1L KITLG SFRP4 DAW1 SP5 P3H2 ZSCAN16 COL11A1 EPAS1 SPATS2L C8orf4 TNFRSF11B HTATIP2 KLRC4 MEOX2 SLIT2 DCLK1 CDH11 LOC650226 ITGA2 S100A6 SALL3 COL14A1 RIPPLY3 KLRC3 TES CAV1 ALDH1A1 C8orf34 ARAP3 TCEAL8 LINC01224 ZKSCAN7 KLHDC9 PEG3-AS1 PHLDA1 SNRPN 04-Mar PHLDB2 BHLHE41 PPM1L RNF128 SLITRK6 MFAP5 CXCL1 CTSF ZNF682 TMEM26 VAV3 HRASLS SEMA3D SNURF ZBTB20 S100A11 LINC00052 CTAG2 SOX2-OT SOX2 ARMCX2 ARMCX6 CD109 KLRC2 EIF4E3 CREB5 HAPLN1 EFEMP1 RNLS OTOGL KLRC1 COL17A1
Grp 1-5	73	TWIST2 MAGEA8 CGREF1 FMR1NB SLC16A1-AS1 FAM183A MYPN GTSF1 KLK6 MOXD1 MMP13 ZIC1 DSCR8 GJA1 HOXB9 LCP1 BLMH CCDC3 C1QTNF9B GBA3 NUDT11 ERV9-1 CFI GNAZ FCRL2 KBTBD11 CNTNAP4 CSAG4 NLRP2 RPS4Y2 HOXC9 GAGE7 IFI44L DDX3Y NXF2 NFE4 LEMD1 NXF5 MAEL PRAME HBE1 QPCT BAMBI RPS4Y1 TNS4 WASF3 CPEB1 LOC101060157 NRP2 COX7B2 DAPP1 PRCAT47 HOXB6 FXYD3 CSAG1 COL8A1 RASEF IFI44 LONRF2 ADIRF METTL7A SIMC1 ARHGAP44 TCEAL9 HBG1 FGFBP1 MIR4697HG KRBOX1 KLHL29 MARCH4. DNALI1 ARNTL2 ZNF595
Grp 1-6	85	CAPN8 RAB38 SLC43A3 LMO3 KRT16P2 KDR CABYR GALNT3 PPP1R14A TMEM158 FAM43B RAMP1 VSIG1 CEACAM6 B3GNT6 MRAS BEX2 ATP2C2 SFTA2 MAGEA2B PLEKHS1 S100A14 RADIL UCA1 HNMT TMPRSS4 NPTX1 RASSF8 MAGEA12 TMPRSS13 SLC34A2 TCN1 LAMB1 IGF2 LGSN KRT4 UCHL1 GPX3 SCG2 C16orf45 C4BPB ANKRD30BP2 HENMT1 LINC00578 ATP8B3 FOXD1 KRT6C LCN2 CEACAM5 PLAC8 DENND5B SNCA TREM1 AZGP1 PRDM13 TWF1 ACSL5 MME GALNT5 RECK PCOLCE2 MALL SCAF11 ARID2 FAM101B ZDBF2 KRT6A CHI3L1 FBP1 ANO6 MACC1 DDX43 LTBR ROBO3 GNB4 GSTM3 BATF KCNQ1 ST14 SFTPA1 SLAMF7 ST6GALNAC1 SALL4 ABCA4 RASSF8-AS1

Table 3. Representation of outcome of Figure 2c i.e., the total number of genes and the names of genes for the groups selected to draw it.

List names	number of elements	number of unique elements
Grp 1-2	198	160
Grp 2-5	198	167
Grp 2-6	198	173
Overall number of unique elements		364
Names	total	elements

Grp 1-2 Grp 2-5 Grp 2-6	30	COL3A1 PAM TM4SF1 CTAG1A UNK MBP SOSTDC1 LIN7A IQCA1 LOC645321 FAM9C SFRP4 COL11A1 EPAS1 SPATS2L HTATIP2 S100A6 TES CAV1 ALDH1A1 TCEAL8 SNRPN MFAP5 SEMA3D SNURF S100A11 LINC00052 CTAG2 ARMCX6 CD109
Grp 1-2 Grp 2-5	8	TMEM35A PRL TEK SAT2 S1PR1 LOC650226 SLITRK6 VAV3
Grp 1-2 Grp 2-6	7	ERBB4 SLC39A8 KCNQ10T1 SULF1 SLIT2 CDH11 RIPPLY3
Grp 2-5 Grp 2-6	61	HDGFRP3 KRT19 LAMB3 PHF21B GALNT3 TMEM45B ZIC1 FGFR1 BEX2 AFAP1-AS1 MAGED4B COL5A2 LY6K LAMC2 S100A14 GJA1 ANXA3 NUDT11 RAC2 CD55 EML1 BMP7 AIM2 CAV2 SFTA3 NEFH DZIP1 HOXC9 BEX3 SLC1A1 ADGRF1 ERP27 ASRGL1 FGF2 MGST2 LAD1 CST6 TACSTD2 CASP4 ATCAY MLPH MALL PNMAL1 TGFB1 CFH TRO BEX4 EPHA5 PRSS23 NKX2-1 HOXB13 HTRA1 ARSJ HCAR1 MGST1 GRIA2 IGF2BP1 TCEAL9 FGFBP1 KRT7 TMEM246
Grp 1-2	115	EMP1 KCNMA1 CYB5R2 CYP26A1 LEF1 STYK1 CDH7 NTSR1 GRAMD1B C15orf48 COL4A5 ZNF93 FBLL1 ZDHHC15 SGK1 CD24 SSPN TUNAR KIAA2022 ZNF667-AS1 PCDH11Y CCND2 BASP1 FAXDC2 SOX21 KIRREL ZNF439 CRH GSG1 ARL14 SEC14L4 DMD CCL20 PDLIM3 ZNF702P PROK2 SCOC CDCP1 ST8SIA6-AS1 TCEAL7 NNT UTS2B RGS17 UTS2 CXCL2 CLDN1 SOX17 VWA5A RGCC TMEM30B ZNF736 ZNF257 DNAJA4 FGF9 CSGALNACT1 FRRS1L KITLG DAW1 SP5 P3H2 ZSCAN16 FOXF2 CDH10 C8orf4 TNFRSF11B KLRC4 MEOX2 DCLK1 GPX1 CX3CL1 ITGA2 SALL3 COL14A1 KLRC3 SCEL TFPI2 C8orf34 HOXB3 ARAP3 LINC01224 ZKSCAN7 KLHDC9 PEG3-AS1 PHLDA1 04-Mar PHLDB2 BHLHE41 PPM1L RNF128 CXCL1 CTSF ZNF682 PRKCQ-AS1 TMEM26 NNMT GSTT1 HRASLS ZBTB20 SOX2-OT SOX2 ARMCX2 GNG11 KLRC2 EIF4E3 PDE4B AGR2 CREB5 HAPLN1 EFEMP1 MAGEA4 RNLS OTOGL SPOCK1 KLRC1 COL17A1
Grp 2-5	68	MAGEA8 FMR1NB GRB10 TNC KRT80 DSCR8 TMSB15A ADRA1B ARHGAP9 MGAT3 RBM20 GFOD1 GPX7 LCP1 BLMH C1QTNF9B ZBED2 SMO PLCB1 SPP1 GLI1 ERV9-1 CFI GNAZ ANK3 MB HS3ST1 NLRP2 RPS4Y2 RBM24 GAGE7 SAMD9 FOXA2 NEO1 MARK1 TMEM98 NXF2 FOXL2 NFE4 TSPYL5 RBP7 NXF5 MAEL PRAME SLCO3A1 LHX2 RPS4Y1 TNS4 AUTS2 WASF3 LOC101060157 INHBB NRP2 COX7B2 CSAG1 MAL2 COL8A1 MAPT BARX1 TP63 IFI44 ADIRF PSD3 ERICH5 ZNF711 CADM1 ARNTL2 ARHGDI3
Grp 2-6	75	MPDZ CASP5 KRT16P2 LINC00839 CABYR MDFIC PPP1R14A KIAA1211 MSRB3 DEPDC7 CEACAM6 MRAS PTPRE VEGFC TUBB2B PCDHB2 SCNN1A RADIL UCA1 HNMT TMPRSS4 SLC34A2 FAM171B PALLD PHGDH ID4 LGSN UCHL1 PLAT NAV2 C4BPB CASC15 ANKRD30BP2 SRPX2 FOXD1 FAM107B PCDHB5 TREM1 KCNQ2 TENM3 AZGP1 PRICKLE1 TWF1 ITGB2 ELF3 G0S2 SPTB FUCA2 PCOLCE2 RBP1 MUC4 C1orf116 NRG1 NELL2 PLOD2 FAM92A1 FAM101B TMEM125 PPARG CHI3L1 STEAP2 ANO6 EVL DDX43 KCNS3 LTBR GNB4 GSTM3 SFTPA1 FN1 ATP10A RPRML ST6GALNAC1 SALL4 SKIDA1

Finally, after comparative analysis of the genes, we also explored the the enriched pathways for the venn diagrams presented in Figure 2d, 2e, and 2f which was presented in Table 4. PI3K-Akt and cytokine signaling were common between all the three groups of urinary bladder cell lines (urinary bladder squamous carcinoma cell line - non-permissive for MVwt, urinary bladder transitional cell carcinoma cell line - non-permissive for MVwt, and urinary bladder grade 3 carcinoma cell line - permissive for MVwt), neuroactive ligand-receptor interaction signaling was common between the two groups (urinary bladder squamous carcinoma cell line - non-permissive for MVwt and urinary bladder grade 3 carcinoma cell line - permissive for MVwt), and ECM, focal adhesion, CAMs, and pluropotency of stem cells signaling were common between two groups (urinary bladder transitional cell carcinoma cell line - non-permissive for MVwt and urinary bladder grade 3 carcinoma cell line - permissive for MVwt). Rap1, leukocyte tranendothelial migration, and regulation of actin cytoskeleton was specific to group 4-7 (urinary bladder transitional cell carcinoma cell line - non-permissive for MVwt and urinary bladder grade 3 carcinoma cell line - permissive for MVwt) and hippo signaling was specific to urinary bladder squamous carcinoma cell line - non-permissive for MVwt (Group 3) and urinary bladder transitional cell carcinoma cell line - non-permissive for MVwt (Group 4). In this case, we observe that ECM, focal adhesion, and CAMs, pluropotency of stem cells signaling were most critical signaling pathways for the groups (urinary bladder transitional cell carcinoma cell line - non-permissive for MVwt and urinary bladder grade 3 carcinoma cell line - permissive for MVwt) (Table 4).

We analyzed the outcome of venn diagram of Figure 2e, focal adhesion and PI3K-Akt signaling pathways were dominantly enriched for all the three groups i.e., lung adenocarcinoma cell line a - non-permissive for MVwt (Group 1), lung adenocarcinoma cell line b - non-permissive for MVwt (Group 2), lung bronchioalveolar carcinoma cell line - permissive for MVwt (Group 5), and human lung papillary adenocarcinoma cell line - permissive for MVwt (Group 6). Wnt signaling was enriched for the groups lung adenocarcinoma cell line a - non-permissive for MVwt (Group 1), lung adenocarcinoma cell line b - non-permissive for MVwt (Group 2), and lung bronchioalveolar carcinoma cell line - permissive for MVwt (Group 5) and cytokine signaling was enriched for lung adenocarcinoma cell line a - non-permissive for MVwt (Group 1), lung adenocarcinoma cell line b - non-permissive for MVwt (Group 2), and human lung papillary adenocarcinoma cell line - permissive for MVwt (Group 6). APC, RAP1, NK cell, cAMP, RAS, TNF, and neuroactive ligand-receptor signaling which mostly associated with immune system were specific to lung adenocarcinoma cell line a - non-permissive for MVwt (Group 1) and lung adenocarcinoma cell line b - non-permissive for MVwt (Group 2). ECM was specifically enriched for lung adenocarcinoma cell line a - non-permissive for MVwt (Group 1) and human lung papillary adenocarcinoma cell line - permissive for MVwt (Group 6) (Table 4).

We also analyzed the outcome of venn diagram of Figure 2f, Ras signaling was enriched for all the groups i.e., lung adenocarcinoma cell line a - non-permissive for MVwt (Group 1), lung adenocarcinoma cell line b - non-permissive for MVwt (Group 2), lung bronchioalveolar carcinoma cell line - permissive for MVwt (Group 5), and lung papillary adenocarcinoma cell line - permissive for MVwt (Group 6). Focal adhesion, PI3K-Akt, Rap1, and cAMP signaling were enriched for lung adenocarcinoma cell line a - non-permissive for MVwt (Group 1), lung adenocarcinoma cell line b - non-permissive for MVwt (Group 2), and lung bronchioalveolar carcinoma cell line - permissive for MVwt (Group 5). APC, Wnt, NK, cytokine, TNF, and neuroactive ligand-receptor signaling were specifically enriched for lung adenocarcinoma cell line a - non-permissive for MVwt (Group 1) and lung adenocarcinoma cell line b - non-permissive for MVwt (Group 2). These pathways are critically associated with immune system and thus, we could say that non-permissive lung adenocarcinoma cell lines are potentially sensitive in the sense of immune system. ECM, MAPK, and regulation of actin cytoskeleton signaling pathways were enriched for the celllines lung adenocarcinoma cell line b - non-permissive for MVwt (Group 2), and lung bronchioalveolar carcinoma cell line - permissive for MVwt (Group 5) (Table 4).

Table 4. Representation of outcome of Figure 2d, 2e, and 2f i.e., the total number of genes and the names of genes for the groups selected to draw it.

Names	Total	Pathways
Grp 3-4 Grp 3-7 Grp 4-7	2	KEGG_04151_Pi3k-akt_signaling_pathway_-_Homo_sapiens_(human) KEGG_04060_Cytokine-cytokine_receptor_interaction
Grp 3-7 Grp 4-7	1	KEGG_04080_Neuroactive_ligand-receptor_interaction
Grp 3-4 Grp 4-7	4	KEGG_04512_ECM-receptor_interaction KEGG_04510_Focal_adhesion KEGG_04514_Cell_adhesion_molecules_(CAMs) KEGG_04550_Signaling_pathways_regulating_pluripotency_of_stem_cells
Grp 4-7	3	KEGG_04015_Rap1_signaling_pathway_-_Homo_sapiens_(human) KEGG_04670_Leukocyte_transendothelial_migration KEGG_04810_Regulation_of_actin_cytoskeleton

Grp 3-4	1	KEGG_04392_Hippo_Signaling_Pathway
Names	Total	Pathways
Grp 1-2 Grp 1-5 Grp 1-6	2	KEGG_04510_Focal_adhesion KEGG_04151_PI3K-Akt_signaling_pathway_-_Homo_sapiens_(human)
Grp 1-2 Grp 1-5	1	KEGG_04310_Wnt_signaling_pathway
Grp 1-2 Grp 1-6	1	KEGG_04060_Cytokine-cytokine_receptor_interaction
Grp 1-2	7	KEGG_04612_Antigen_processing_and_presentation KEGG_04015_Rap1_signaling_pathway_-_Homo_sapiens_(human) KEGG_04650_Natural_killer_cell_mediated_cytotoxicity KEGG_04024_cAMP_signaling_pathway_-_Homo_sapiens_(human) KEGG_04014_Ras_signaling_pathway_-_Homo_sapiens_(human) KEGG_04668_TNF_signaling_pathway_-_Homo_sapiens_(human) KEGG_04080_Neuroactive_ligand-receptor_interaction
Grp 1-6	1	KEGG_04512_ECM-receptor_interaction
Names	Total	Pathways
Grp 1-2 Grp 2-5 Grp 2-6	1	KEGG_04014_Ras_signaling_pathway_-_Homo_sapiens_(human)
Grp 1-2 Grp 2-5	4	KEGG_04510_Focal_adhesion KEGG_04015_Rap1_signaling_pathway_-_Homo_sapiens_(human) KEGG_04151_PI3K-Akt_signaling_pathway_-_Homo_sapiens_(human) KEGG_04024_cAMP_signaling_pathway_-_Homo_sapiens_(human)
Grp 1-2	6	KEGG_04612_Antigen_processing_and_presentation KEGG_04310_Wnt_signaling_pathway KEGG_04650_Natural_killer_cell_mediated_cytotoxicity KEGG_04060_Cytokine-cytokine_receptor_interaction KEGG_04668_TNF_signaling_pathway_-_Homo_sapiens_(human) KEGG_04080_Neuroactive_ligand-receptor_interaction
Grp 2-5	3	KEGG_04512_ECM-receptor_interaction KEGG_04810_Regulation_of_actin_cytoskeleton KEGG_04010_MAPK_signaling_pathway

4. Discussion: In this study, we presented the comparative analysis of gene expression and pathway enrichment analysis different cell lines for the purpose to understand the measles infection (MV) impact on immune system. All three groups of urinary bladder cell lines shared PI3K-Akt and cytokine signaling (Urinary Bladder Squamous Carcinoma Cell Line: Non-permissive for MVwt, Urinary Bladder Transitional Cell Carcinoma Cell Line: Non-permissive for MVwt, and Urinary Bladder Grade 3 Carcinoma Cell Line: Permissive for MVwt). Neuroactive ligand-receptor interaction signaling was shared by the two groups (Urinary Bladder Squamous carcinoma cell line: non-permissive for MVwt and Urinary Bladder Grade 3 Cell Line: Permissive for MVwt), and ECM, focal adhesion, CAMs, and pluripotency of stem cell signaling were shared by the two groups (Urinary Bladder Transitional Cell Carcinoma Cell Line: Non-permissive for MVwt and Urinary Bladder Grade 3 Cell Line: Permissive for MVwt). Hippocampal signaling was unique to the urinary bladder squamous carcinoma cell line, which was non-permissive for MVwt (Group 3), and the urinary bladder transitional cell carcinoma cell line, which was non-permissive for MVwt (Group 4). Rap1, leukocyte tranendothelial migration, and regulation of actin cytoskeleton were specific to groups 4-7 (urinary bladder transitional cell carcinoma cell line - non-permissive for MVwt and urinary bladder grade 3 carcinoma cell line - permissive for MVwt). In this instance, we find that the most important signaling pathways for the groups (urinary bladder transitional cell carcinoma cell line, which is not permissive for MVwt, and urinary bladder grade 3 carcinoma cell line, which is permissive for MVwt) were ECM, focal adhesion, and CAMs, as well as pluripotency of stem cells (Table 4). APC, RAP1, NK cells, cAMP, RAS, TNF, and neuroactive ligand-receptor signaling—all of which are primarily linked to the immune system—were unique to lung adenocarcinoma cell lines a and b, which are non-permissive for MVwt (Group 1 and Group 2, respectively). Particularly, ECM was enriched for human lung papillary adenocarcinoma cell line a, which is permissive

for MVwt (Group 6), and lung adenocarcinoma cell line a, which is non-permissive for MVwt (Group 1). For lung adenocarcinoma cell line a, which is non-permissive for MVwt (Group 1), lung adenocarcinoma cell line b, which is non-permissive for MVwt (Group 2), and lung bronchioalveolar carcinoma cell line, which is permissive for MVwt (Group 5), focal adhesion, PI3K-Akt, Rap1, and cAMP signaling were enriched. In particular, lung adenocarcinoma cell line a—which is non-permissive for MVwt (Group 1)—and lung adenocarcinoma cell line b—which is non-permissive for MVwt (Group 2)—had higher levels of APC, Wnt, NK, cytokines, TNF, and neuroactive ligand-receptor signaling. Since these pathways are closely linked to the immune system, we may conclude that non-permissive lung adenocarcinoma cell lines may be immune system-sensitive. For the cell lines lung adenocarcinoma cell line b, which is non-permissive for MVwt (Group 2), and lung bronchioalveolar carcinoma cell line, which is permissive for MVwt (Group 5), ECM, MAPK, and modulation of actin cytoskeleton signaling pathways were enriched.

The most contagious virus in humans is the measles virus (MV). When MV enters a new host, it does not immediately infect epithelial cells like the majority of respiratory viruses do. MV travels via immune cells' epithelium before being sent to lymphatic organs for multiplication. Large volumes of virus are then concurrently delivered to the airways by infected immune cells. Nevertheless, nothing is known about MV replication in airway epithelia. Previously[32], it was modeled by using primary cultures of human airway epithelial cells (HAE) from lung donors that have undergone proper differentiation. MV transmits directly from cell to cell in HAE, creating infectious foci that develop for three to five days, stabilize for a few days, and then vanish. We postulated that MV infectious centers may dislodge while epithelial function is maintained because transepithelial electrical resistance does not change over the duration of HAE infection. Following confocal microscopy's confirmation that infectious centers gradually split from HAE, they retrieved apical washes and used centrifugation to separate the virus's cell-associated and cell-free components. Compared to the supernatant, the virus titers in the cell-associated fraction were almost ten times higher. Ciliary beating continued and apoptotic markers were not easily found in displaced infection centers, indicating that they still have functional metabolism.

Nectin-4 is known to be expressed by lung cancer cells, especially those of non-small-cell lung cancer. We previously created a recombinant measles virus that can engage its primary receptor, signaling lymphocyte activation molecule (SLAM), but is unable to bind Nectin-4. In vitro and in a subcutaneous xenograft form, this virus (rMV-SLAMblind) infects and destroys breast cancer cells. The effectiveness of rMV-SLAMblind against additional cancer types and in other tumor models that more accurately reflect illness has not yet been established. Using a modified version of the virus that encodes green fluorescent protein (rMV-EGFP-SLAMblind), the anti-tumor effect of this virus against lung cancer cells was examined in earlier research. They discovered that nine human lung cancer cell lines were effectively infected by rMV-EGFP-SLAMblind, and that six of the cell lines had decreased viability as a result of the infection. When the virus was administered to xenotransplanted mice's subcutaneous tumors, the growth of the tumor was inhibited. Furthermore, the lungs of xenotransplanted mice may harbor dispersed tumor masses that rMV-EGFP-SLAMblind could target. According to these findings, rMV-SLAMblind is an oncolytic for lung cancer and has promise as a treatment for this illness[23, 33, 34]. In the previous work, so far there are limited study in this regards, thus, we uniquely presented our study to explore the DEGs and enriched pathways mutually common or exclusively cell line specific for which we utilized the dataset freely available in different types of cell lines.

5. Conclusions: In conclusion, we found that lung adenocarcinoma cell line a was non-permissive for MVwt, while lung adenocarcinoma cell line b was non-permissive for MVwt. These factors were specifically related to the immune system and included APC, RAP1, NK cells, cAMP, RAS, TNF, and neuroactive ligand-receptor signaling. ECM was particularly enriched for human lung papillary adenocarcinoma cell line, which is permissive for MVwt, and lung adenocarcinoma cell line a, which is non-permissive for MVwt. For lung adenocarcinoma cell line a, which is non-permissive for MVwt, lung adenocarcinoma cell line b, which is non-permissive for MVwt, and lung bronchioalveolar carcinoma cell line, which is permissive for MVwt, focal adhesion, PI3K-Akt, Rap1, and cAMP signaling were enriched. For lung adenocarcinoma cell line a, which is non-permissive for MVwt, and lung adenocarcinoma cell line b, which is non-permissive for MVwt, there was a distinct enrichment of APC, Wnt, NK, cytokine, TNF, and neuroactive ligand-receptor signaling. Since these pathways are closely linked to the immune system, we may conclude that non-permissive lung adenocarcinoma cell lines may be immune system-sensitive. The cell lines lung adenocarcinoma cell line b, which is non-permissive for MVwt, and lung bronchioalveolar carcinoma cell line, which is permissive for MVwt, were shown to have enriched ECM, MAPK, and modulation of actin cytoskeleton signaling pathways.

Author Contributions: Conceptualization, S.I. and M.T.; methodology, S.I. and M.T.; software, S.I. and M.T.; validation, S.I. and M.T.; formal analysis, S.I. and M.T.; investigation, S.I.; resources, S.I.; data curation, S.I.; writing—original draft preparation, S.I. and M.T.; writing—review and editing, S.I. and M.T.; visualization, S.I.; supervision, S.I.; project administration, S.I.; funding acquisition, S.I. and M.T. All authors have read and agreed to the published version of the manuscript.

Funding: Not applicable.

Acknowledgments: We are grateful to the Department of Biotechnology, Faculty of Natural Science, Norwegian University of Science and Technology, Trondheim 7491, Norway for providing us all the facilities to carry out the entire work.

Conflicts of Interest: The authors declare no conflict of interest. The funders had no role in the design of the study; in the collection, analyses, or interpretation of data; in the writing of the manuscript, or in the decision to publish the results.

Institutional Review Board Statement: Not applicable.

Informed Consent Statement: Not applicable.

Data Availability Statement: All the related data are supplied in this work or have been referenced properly.

References

1. Bredin, C.G., et al., *Integrin dependent migration of lung cancer cells to extracellular matrix components*. Eur Respir J, 1998. **11**(2): p. 400-7.
2. Chen, Z., et al., *Non-small-cell lung cancers: a heterogeneous set of diseases*. Nature Reviews Cancer, 2014. **14**(8): p. 535-546.
3. Daniels, M., et al., *Whole genome sequencing for lung cancer*. Journal of Thoracic Disease, 2012. **4**(2): p. 155-63.
4. Guan, P., et al., *Lung cancer gene expression database analysis incorporating prior knowledge with support vector machine-based classification method*. Journal of Experimental & Clinical Cancer Research, 2009. **28**(1): p. 103.
5. Bray, F., et al., *Global cancer statistics 2022: GLOBOCAN estimates of incidence and mortality worldwide for 36 cancers in 185 countries*. CA Cancer J Clin, 2024. **74**(3): p. 229-263.
6. Leonard, V.H., et al., *Measles virus blind to its epithelial cell receptor remains virulent in rhesus monkeys but cannot cross the airway epithelium and is not shed*. J Clin Invest, 2008. **118**(7): p. 2448-58.
7. Morgan, E.M. and F. Rapp, *Measles virus and its associated diseases*. Bacteriol Rev, 1977. **41**(3): p. 636-66.
8. Fielding, A.K., *Measles as a potential oncolytic virus*. Rev Med Virol, 2005. **15**(2): p. 135-42.
9. Yanagi, Y., M. Takeda, and S. Ohno, *Measles virus: cellular receptors, tropism and pathogenesis*. J Gen Virol, 2006. **87**(Pt 10): p. 2767-2779.
10. Guseva, S., et al., *Structure, dynamics and phase separation of measles virus RNA replication machinery*. Curr Opin Virol, 2020. **41**: p. 59-67.
11. Sion-Vardy, N., et al., *Measles virus: evidence for association with lung cancer*. Exp Lung Res, 2009. **35**(8): p. 701-12.
12. Smok-Kalwat, J., et al., *The Importance of the Immune System and Molecular Cell Signaling Pathways in the Pathogenesis and Progression of Lung Cancer*. Int J Mol Sci, 2023. **24**(2).
13. Bajrai, L.H., et al., *Understanding the role of potential pathways and its components including hypoxia and immune system in case of oral cancer*. Sci Rep, 2021. **11**(1): p. 19576.
14. Edwards, S.C., W.H.M. Hoevenaar, and S.B. Coffelt, *Emerging immunotherapies for metastasis*. British Journal of Cancer, 2021. **124**(1): p. 37-48.
15. El-Kafrawy, S.A., et al., *Genomic profiling and network-level understanding uncover the potential genes and the pathways in hepatocellular carcinoma*. Front Genet, 2022. **13**: p. 880440.
16. Netea, M.G., et al., *Defining trained immunity and its role in health and disease*. Nat Rev Immunol, 2020. **20**(6): p. 375-388.
17. Baba, M.R. and S.A. Buch, *Revisiting Cancer Cachexia: Pathogenesis, Diagnosis, and Current Treatment Approaches*. Asia-Pacific Journal of Oncology Nursing, 2021. **8**(5): p. 508-518.
18. Chen, K., et al., *PD-L1 expression and T cells infiltration in patients with uncommon EGFR-mutant non-small cell lung cancer and the response to immunotherapy*. Lung Cancer, 2020. **142**: p. 98-105.
19. Cui, Q., et al., *A map of human cancer signaling*. Molecular Systems Biology, 2007. **3**(1): p. 152.
20. Gadgeel, S.M. and A. Wozniak, *Preclinical Rationale for PI3K/Akt/mTOR Pathway Inhibitors as Therapy for Epidermal Growth Factor Receptor Inhibitor-Resistant Non-Small-Cell Lung Cancer*. Clinical Lung Cancer, 2013. **14**(4): p. 322-332.
21. Galluzzi, L., et al., *Molecular mechanisms of cell death: recommendations of the Nomenclature Committee on Cell Death 2018*. Cell Death Differ, 2018. **25**(3): p. 486-541.
22. Guo, L., et al., *PD-1/L1 With or Without CTLA-4 Inhibitors Versus Chemotherapy in Advanced Non-Small Cell Lung Cancer*. Cancer Control, 2022. **29**: p. 10732748221107590.
23. Muhlebach, M.D., et al., *Adherens junction protein nectin-4 is the epithelial receptor for measles virus*. Nature, 2011. **480**(7378): p. 530-3.
24. Barrett, T., et al., *NCBI GEO: archive for functional genomics data sets--update*. Nucleic Acids Res, 2013. **41**(Database issue): p. D991-5.
25. Almowallad, S., R. Jeet, and M. Mobashir, *A systems pharmacology approach for targeted study of potential inflammatory pathways and their genes in atherosclerosis*. Jour. Bas. Sci., 2024. **6**(1): p. 1-12.

26. Choudhry, H., et al., *Study of APOBEC3B focused breast cancer pathways and the clinical relevance*. Jour. Bas. Sci., 2024. **2**(1): p. 1-12.
27. Khan, B. and M.M.A. Rizv, *San Huang Decoction as an effective treatment for oral squamous cell carcinoma based on network pharmacology*. Jour. Bas. Sci., 2025. **4**(2): p. 1-17.
28. Mobashir, M., et al., *An Approach for Systems-Level Understanding of Prostate Cancer from High-Throughput Data Integration to Pathway Modeling and Simulation*. Cells, 2022. **11**(24).
29. Anwer, S.T., et al., *Synthesis of Silver Nano Particles Using Myricetin and the In-Vitro Assessment of Anti-Colorectal Cancer Activity: In-Silico Integration*. Int J Mol Sci, 2022. **23**(19).
30. Bajrai, L.H., et al., *Gene Expression Profiling of Early Acute Febrile Stage of Dengue Infection and Its Comparative Analysis With Streptococcus pneumoniae Infection*. Front Cell Infect Microbiol, 2021. **11**: p. 707905.
31. Eldakhakhny, B.M., et al., *In-Silico Study of Immune System Associated Genes in Case of Type-2 Diabetes With Insulin Action and Resistance, and/or Obesity*. Front Endocrinol (Lausanne), 2021. **12**: p. 641888.
32. Hippee, C.E., et al., *Measles virus exits human airway epithelia within dislodged metabolically active infectious centers*. PLoS Pathog, 2021. **17**(8): p. e1009458.
33. Fujiyuki, T., et al., *A measles virus selectively blind to signaling lymphocytic activation molecule shows anti-tumor activity against lung cancer cells*. Oncotarget, 2015. **6**(28): p. 24895-903.
34. Tamura, K., et al., *Anti-tumor activity of a recombinant measles virus against canine lung cancer cells*. Sci Rep, 2023. **13**(1): p. 18168.

Disclaimer/Publisher's Note: The statements, opinions and data contained in all publications are solely those of the individual author(s) and contributor(s) and not of Global Journal of Basic Science and/or the editor(s). Global Journal of Basic Science and/or the editor(s) disclaim responsibility for any injury to people or property resulting from any ideas, methods, instructions or products referred to in the content.

Copyright: © 2025 by the authors. Submitted for possible open access publication under the terms and conditions of the Creative Commons Attribution (CC BY) license (<https://creativecommons.org/licenses/by/4.0/>).